

## Evaluation of a Foam Buffer Target Design for Spatially Uniform Ablation of Laser-Irradiated Plasmas

M. Dunne,\* M. Borghesi, A. Iwase, M. W. Jones, R. Taylor, and O. Willi

*Imperial College of Science, Technology, and Medicine, London, SW7 2BZ, United Kingdom*

R. Gibson, S. R. Goldman, J. Mack, and R. G. Watt

*Los Alamos National Laboratory, Los Alamos, New Mexico 87545*

(Received 8 March 1995)

Experimental observations are presented demonstrating that the use of a gold-coated foam layer on the surface of a laser-driven target substantially reduces its hydrodynamic breakup during the acceleration phase. The data suggest that this results from enhanced thermal smoothing during the early-time imprint stage of the interaction. The target's kinetic energy and the level of parametric instability growth are shown to remain essentially unchanged from that of a conventionally driven target.

PACS numbers: 52.50.Jm, 52.25.Nr, 52.40.Nk

A prime contender for a viable inertial confinement fusion (ICF) driver is direct illumination by a large number of high power optical laser beams. This scheme has the benefits of geometrical simplicity and potentially high overall energy efficiency. However, the wave front of such a high power laser beam can suffer from severe and unpredictable intensity nonuniformities. These lead to nonuniform energy deposition and the seeding of a number of deleterious instabilities in the underdense and overdense plasmas. To date, laser-based techniques have proved inadequate in overcoming the imprinting of intensity nonuniformities in the early-time "startup" phase of the laser-target interaction [1,2]. In all such smoothing schemes the instantaneous laser intensity profile remains grossly nonuniform, with effective smoothing occurring only over a large number of coherence times. The proximity of the absorption region to the ablation surface in the initial plasma means that there is an insufficient distance over which transverse *thermal* smoothing of the nonuniform imprint can occur before it reaches the ablation surface [2,3]. The mass flow perturbations induced by this imprinting can far outweigh those arising from the surface roughness of the target and act to reduce the distance over which a target can be accelerated before breakup. This effect imposes a severe limit on the maximum allowed aspect ratio of a fusion capsule and would therefore limit the thermonuclear yield attainable by laser fusion [4].

It has been demonstrated [1] that the presence of an x-ray preformed plasma buffer in front of a target surface can act to smooth laser nonuniformities and result in uniform ablation as long as the distance between the absorption and ablation surfaces is greater than the perturbation wavelength. The production of this preformed buffer by direct x-ray illumination of a solid target may, however, be unsatisfactory for the purposes of ICF. Specifically, the x-ray preforming process does not allow sufficient scope for tailoring the plasma buffer. A

large subcritical plasma will exist between the drive laser and the solid shell, providing a fertile environment for the growth of parametric instabilities. In addition, the high intensity and extended pulse length of the initial x-ray burst needed to form the required plasma scale lengths will induce hydrodynamic motion well ahead of the ablative shock wave, possibly leading to decompression of the pusher and preheating of the inner cryogenic fuel.

A computational design study of this outstanding problem led us to propose a solution in which the x-ray burst is incident onto a thin, low density foam layer overcoated on the solid target surface [5]. The x-ray heating can then occur through the passage of a supersonic, isochoric ionization wave, thus preventing any hydrodynamic disturbance reaching the fuel interface prior to the thermal front induced by the main drive laser. The supersonic production of supercritical, homogenous plasmas from x-ray irradiated foam layers has already been demonstrated [6]. The initial distance between the critical and ablation surfaces is approximately set by the thickness of the overcoated foam layer, with an insignificant amount of underdense plasma created during the initial x-ray period. The foam buffer is introduced to influence only the initial ( $t < 500$  ps) startup phase of the interaction. The use of such a compound target design has applications in any situation where the integrity of a laser-accelerated foil has to be maintained, or where it is desirable to produce a smooth thermal front in a static target. The term "foam buffered direct drive" (FDD) is adopted for the scheme.

This Letter now aims to establish experimentally the validity of the proposed smoothing scheme. Two series of experiments were performed on separate laser systems, with good agreement between two large data sets obtained. Results representative of the combined experiments will be presented. The first series was performed on the TRIDENT glass laser at Los Alamos using a single second harmonic beam ( $\lambda = 0.53 \mu\text{m}$ ,  $f/6$  optics) to heat and drive the target. The second series was con-

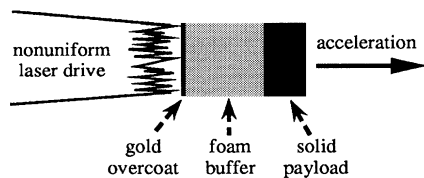


FIG. 1. Schematic of the main target geometry.

ducted on the VULCAN glass laser at the Central Laser Facility. Here a seven-beam, second harmonic  $f/10$  cluster configuration irradiated the target, including an axial beam from which backscattered light levels were monitored. Irradiances in the range  $(1-5) \times 10^{14} \text{ W cm}^{-2}$  were achieved in a  $300 \mu\text{m}$  diameter focal spot using a flat-top pulse of 1.5 ns FWHM duration, with a 100 ps rise time and a falling edge extending to 2–2.5 ns. Coherent beams were used to present the most taxing irradiation conditions for the smoothing scheme.

The targets used consisted of 1 mm diameter triacrylate ( $\text{C}_{15}\text{H}_{20}\text{O}_6$ ) foam cylinders [7],  $50 \text{ mg/cm}^3$  in density and  $50 \mu\text{m}$  thickness, formed onto  $10.6 \mu\text{m}$  thick solid parylene-N ( $\text{C}_8\text{H}_8$ ) or Mylar ( $\text{C}_{10}\text{H}_4\text{O}_8$ ) foils. Polymerization of the foam layer directly onto the solid foil ensured that a uniform and intimate contact between the two regions was achieved. Cell sizes in the foam were of order  $1 \mu\text{m}$  in diameter. These targets were then overcoated with  $250 \text{ \AA}$  gold on the laser side. This overcoat acted to produce a supersonic x-ray ionization wave dur-

ing the leading edge of the drive pulse, which was observed to preform the foam layer. The target irradiation geometry is shown schematically in Fig. 1. The simplicity of such a target design should allow a relatively easy conversion to spherical geometry.

A face-on extreme ultraviolet (XUV) radiography technique [8] (operating at  $50 \text{ \AA}$  with a  $5 \text{ \AA}$  bandwidth and at a magnification of  $80\times$ ) imaged the response of the targets to the laser interaction. The detector was a 2D gated microchannel plate imager (four time frames with 120 ps gate time), which monitored the relative transmission of the target to x rays emanating from a separate gold disk irradiated at  $10^{14} \text{ W cm}^{-2}$ . Self-emission from the foils was shown to be negligible. The modulation transfer function was measured from static backlit grids, being well approximated by a curve of the form  $\exp(-k^2\sigma^2/2)$ , where  $k$  is the perturbation wave number and  $\sigma$  is the standard deviation equal to  $2.3 \mu\text{m}$  at best focus and  $3.3 \mu\text{m}$  at the maximum displacement of the accelerating targets ( $125 \mu\text{m}$ ). Figure 2 illustrates the response of a directly driven solid foil in comparison to an FDD target towards the end of the laser pulse. In the case of the conventional plain foil, gross nonuniformities were observed throughout the acceleration period. These resulted from laser nonuniformities imprinting onto the solid surface before a sufficient critical-to-ablation distance had been formed. The hard ring on the edge of the TRIDENT beam was clearly reproduced onto the foil, producing transmission variations greater than a factor of 4 over scale lengths of  $30-60 \mu\text{m}$ . The raw data were processed by convert-

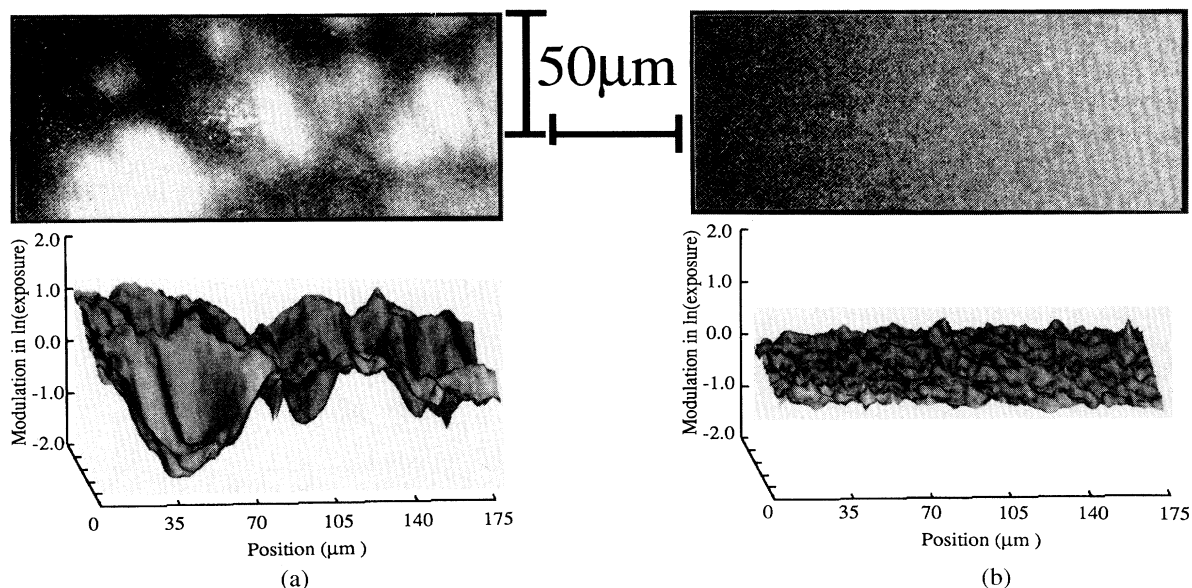


FIG. 2. Face-on 2D XUV radiographs and corresponding modulations in  $\ln(\text{exposure})$  across (a) a conventional,  $10.6 \mu\text{m}$  thick solid  $\text{C}_8\text{H}_8$  foil target, (b) an "FDD" target consisting of a gold-coated,  $50 \mu\text{m}$  thick triacrylate foam layer on a  $10.6 \mu\text{m}$  thick solid  $\text{C}_8\text{H}_8$  foil. These measurements were taken at  $2.1 \pm 0.2 \text{ ns}$  and sample one quarter of the focal spot profile of a coherent beam. Peak irradiance was  $(1.0 \pm 0.5) \times 10^{14} \text{ W cm}^{-2}$ .

ing the nonlinear film density to exposure; the detector response and backlighter falloff were then accounted for and the natural logarithm taken to obtain  $\ln(\text{exposure})$ . The variation of this parameter ( $\approx$  optical depth modulations [9]) was quantified by calculating its standard deviation ( $\sigma$ ). For the plain foil,  $\sigma = 0.58 \pm 0.11$  at 2.2 ns. Detector noise of the order of 0.1, primarily on a spatial scale comparable to the resolution limit of the imaging system. In contrast, images taken using the FDD targets and identical irradiation conditions presented a far more uniform profile, with  $\sigma = 0.12 \pm 0.02$  at 2.1 ns. Fourier analysis of these data illustrated that growth occurred on the characteristic laser perturbation scale lengths; expressed as an exponential growth rate, values for individual modes fell in the range  $(0.3\text{--}1.6) \times 10^9 \text{ s}^{-1}$  for wavelengths of 6 to 30  $\mu\text{m}$  between 0.9 and 1.5 ns. Growth in the plain foil was observed to follow the same behavior over a similar time scale (although at larger modulation amplitudes due to the additional imprint seed).

It is useful to estimate the sensitivity to areal density perturbations from the above measurements, since this parameter excludes the material opacity. Hydrocode simulations (as in [5]) postprocessed by the detailed opacity code IMP [10] agreed with measured estimates of the accelerating target transmission and were consequently used to infer areal density sensitivities. The sensitivity exhibited a steady falloff with time due to a reduction in optical depth of the ablating targets. Before shock breakout, areal density modulations of 2% of the total were predicted to be detectable in the FDD foils, rising to 8% at 2 ns. Slightly improved sensitivities were predicted for the plain foils (up to a factor of 2 better at  $0.9 \pm 0.2$  ns), although for early ( $t < 0.4$  ns) and late ( $t > 1.4$  ns) times the values closely matched those of the FDD foils, indicating that direct comparison of the radiographic data in Fig. 2 is permissible.

An additional series of measurements was obtained on foam buffered, premodulated targets in which the smoothed laser drive was used to analyze Rayleigh-Taylor growth seeded almost exclusively from target perturbations. Modulations were observed throughout the interaction for wavelengths down to 12  $\mu\text{m}$ . These data will be presented in detail elsewhere. Measurements were also taken using aluminum-coated  $\text{C}_8\text{H}_8$  foils, which showed the same characteristic XUV transmission profile as the data set described above and so established that early-time shinethrough of laser light in the optically transparent plain foils was not a significant contributory factor in their hydrodynamic breakup. Similarly, any differences in lateral transport on the rear surfaces of plain and FDD targets are predicted to be small. Finally, imprint data on gold-coated  $\text{C}_8\text{H}_8$  foils were obtained, which demonstrated that radiative preheating of the plastic foil was not the principal mechanism responsible for the reduction in the level of laser imprinting.

It is suggested, therefore, that the observed smoothing arises from thermal transport effects as the laser-induced

shock front propagates through the preheated, long scale length, supercritical plasma (created by the passage of the x-ray precursor through the foam layer). During this period, the critical surface is separated from the solid surface by a distance of the order of the thickness of the foam overcoat. Without a precursor x-ray ionization wave the scale lengths, absolute temperature, and foam uniformity ahead of the laser-induced shock will all be substantially reduced, limiting the scope for thermal smoothing. This is reflected in the data. Side-on XUV imaging was used to record the uniformity of the heat front propagating through gold-coated and -uncoated foam targets. Intense self-emission filaments and a nonuniform absorption profile were observed in uncoated foam targets, whereas the self-emission was substantially smoother for the gold-coated foams, with an absorption front smooth to within the 5  $\mu\text{m}$  spatial resolution of this side-on system. Face-on measurements of uncoated foam-foil targets showed breakup on scale lengths of 5–10  $\mu\text{m}$  ( $\sigma = 0.36 \pm 0.1$  at 1.2 ns).

This laser interaction with gold-coated and uncoated foam targets has been analyzed using LASNEX [11] in 2D. A target of density 50  $\text{mg}/\text{cm}^3$  was simulated using SESAME equation of state data for carbon phenolic, with and without a 250  $\text{\AA}$  gold overcoat. No attempt was made to model the cellular structure of the foam. A 100 ps rise to  $2 \times 10^{14} \text{ W cm}^{-2}$  and a 200  $\mu\text{m}$  diameter spot were used. For the gold-coated foam, the propagation of a radiatively driven ionization front was observed in front of an ablatively driven shock wave in the initial interaction. At 100 ps an electron density scale length of 35  $\mu\text{m}$  was seen in the foam region *ahead* of the shock wave, with the 50 eV temperature contour situated roughly 15  $\mu\text{m}$  ahead of the density peak. At this time, the critical density surface of the driving laser had just penetrated the gold-foam interface, 10  $\mu\text{m}$  behind the density peak (i.e., 7  $\mu\text{m}$  into the foam). Similar behavior can be expected for third harmonic light. Without the gold layer, the density scale length was reduced to

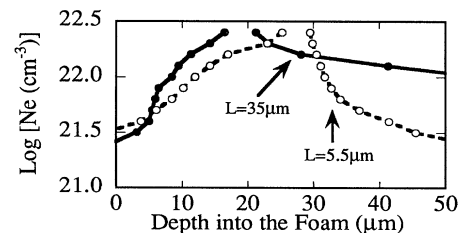


FIG. 3. Results from 2D LASNEX simulations of the behavior of a gold-coated plastic "foam" buffer layer ( $-\bullet-$ ) in comparison to an uncoated "foam" ( $--\circ--$ ). On axis electron density profiles are shown at 100 ps into the interaction. The difference in scale length ahead of the shock is of interest for the thermal smoothing. Temperature profiles show similar behavior. The initial laser-side surface was at 0  $\mu\text{m}$ .

5.5  $\mu\text{m}$  (see Fig. 3), with no evidence of a precursor wave. Simulations were also performed for plain and foam buffered solid targets, using either 10  $\mu\text{m}$  of plastic or 6  $\mu\text{m}$  of aluminum for the foil. For times greater than 1 ns, severe density perturbations on a scale of the imposed laser nonuniformity (30  $\mu\text{m}$ ) existed in the plain foils, whereas a smooth density profile was observed for the foam buffered foils due to smoothing of the nonuniform shock in the foam layer, in good agreement with experimental observations.

Effective thermal smoothing is of limited use, however, if it compromises the efficiency with which a target can be accelerated. The trajectories of FDD and plain-foil targets (Fig. 4) were monitored on separate shots using side-on XUV streak records, as in [12]. The velocity of the center of each foil closely followed the velocity of the rear edges, indicating the lack of any substantial target decompression. Such observations are consistent with the detailed hydrocode simulations of the interactions, in which the payload kinetic energy remained essentially unaffected by the addition of a foam overcoat. The retention of hydrodynamic efficiency is readily understood by considering that in an interaction with a solid foil, the distance between the critical and ablation surfaces reaches a steady-state value of 20–50  $\mu\text{m}$  within the first few hundred picoseconds, whereas the foam buffer merely imposes this separation from the start of the interaction. Early-time x-ray preheat of the solid foils was also shown to be relatively insignificant in these simulations, with the weak x-ray induced shock wave overtaken by the ablatively driven shock before breakout. For the thinner targets used in Fig. 2, there was a short period (<100 ps) of decompression, resulting in a rise in the FDD-foil adiabat during the acceleration period by roughly a factor of 2 over the plain foil value.

These results provide an indication that little energy is lost to parametric processes occurring in the preformed plasma. Confirmation was obtained using calibrated, time-resolved diodes, which demonstrated that less than

5% of the incident laser energy was lost to stimulated Brillouin scattering (collected in the focusing optic). This is in comparison to 3% losses that resulted from interactions with a plain, solid  $\text{C}_8\text{H}_8$  foil. Using the  $f/10$  system, the absolute levels of Brillouin and Raman scattering and their spectral characteristics were also shown to remain essentially unchanged, with absolute values consistently lower than for the  $f/6$  interactions quoted above.

In summary, we have demonstrated that an x-ray preformed foam buffer layer is capable of removing laser nonuniformities even from a coherent beam, without compromising the hydrodynamic performance of the target. These results appear to be encouraging for the prospects of direct-drive ICF, demonstrating a possible means of mitigating one of the primary limiting factors of the viability of high aspect ratio pellets. It now remains to convert these proof-of-principle experiments to spherical implosion. For longer pulse lengths, it may prove necessary to combine this scheme with conventional optical smoothing techniques, given that the steady-state plasma scale lengths may be too small to allow efficient smoothing of static laser nonuniformities [3,5]. Development of a high-gain foam buffered pellet will require further work to reconcile the need to preform the foam buffer with the requirement that the payload be kept on a relatively low adiabat.

Thanks are due to M. Desselberger and T. Afshar-rad for valuable preliminary work; R. Mason, R. Kopp, and H. Vu for ongoing computational analysis; W. Nazarov, J. Falconer, and G. Lyall (Dundee University) and the LANL target fabrication team for supplying the foam; the staff of the CLF for help during the VULCAN experiments. The TRIDENT experiments would not have been possible without the support of J. Faulkner, T. Hurry, B. Boggs, and the entire laser team. This work was partly funded by the EPSRC/MoD.

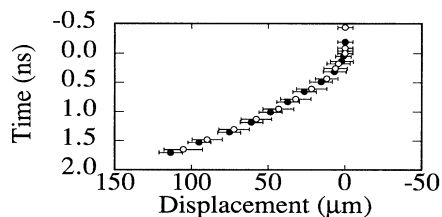


FIG. 4. Comparison of the trajectory of the rear side of a directly driven 12  $\mu\text{m}$  thick solid Mylar foil (solid circles) with an FDD target (open circles) consisting of a 50  $\text{mg}/\text{cm}^3$  foam, 50  $\mu\text{m}$  in length, supported on a 12  $\mu\text{m}$  Mylar foil. Peak irradiance was  $(1.0 \pm 0.5) \times 10^{14} \text{ W cm}^{-2}$ . Shock breakout is normalized to  $t = 0$  for each shot to account for the 150 ps delay induced by the foam buffer. The errors arise primarily from photocathode noise and any initial target tilt.

\*Present address: AWE, Aldermaston, United Kingdom.

- [1] M. Desselberger *et al.*, Phys. Rev. Lett. **68**, 1539 (1992).
- [2] M. H. Emery *et al.*, Phys. Fluids B **3**, 2640 (1991).
- [3] J. H. Gardner and S. E. Bodner, Phys. Rev. Lett. **47**, 1137 (1981).
- [4] J. D. Lindl and W. C. Mead, Phys. Rev. Lett. **34**, 1273 (1975); J. Grun *et al.*, Phys. Rev. Lett. **58**, 2672 (1987); S. G. Glendinning *et al.*, Phys. Rev. Lett. **69**, 1201 (1992).
- [5] M. Desselberger *et al.*, Phys. Rev. Lett. **74**, 2961 (1995).
- [6] T. Afshar-rad *et al.*, Phys. Rev. Lett. **73**, 74 (1994).
- [7] J. Falconer *et al.*, J. Vac. Sci. Technol. A **8**, 968 (1990).
- [8] R. Taylor *et al.* (to be published); O. Willi *et al.*, Rev. Sci. Instrum. **63**, 4818 (1992).
- [9] B. Remington *et al.*, Phys. Plasmas **2**, 241 (1995).
- [10] S. J. Rose, J. Phys. B **25**, 1667 (1992).
- [11] G. B. Zimmerman and W. L. Kruer, Comments Plasma Phys. **2**, 51 (1975).
- [12] J. Edwards *et al.*, Phys. Rev. Lett. **71**, 3477 (1993).

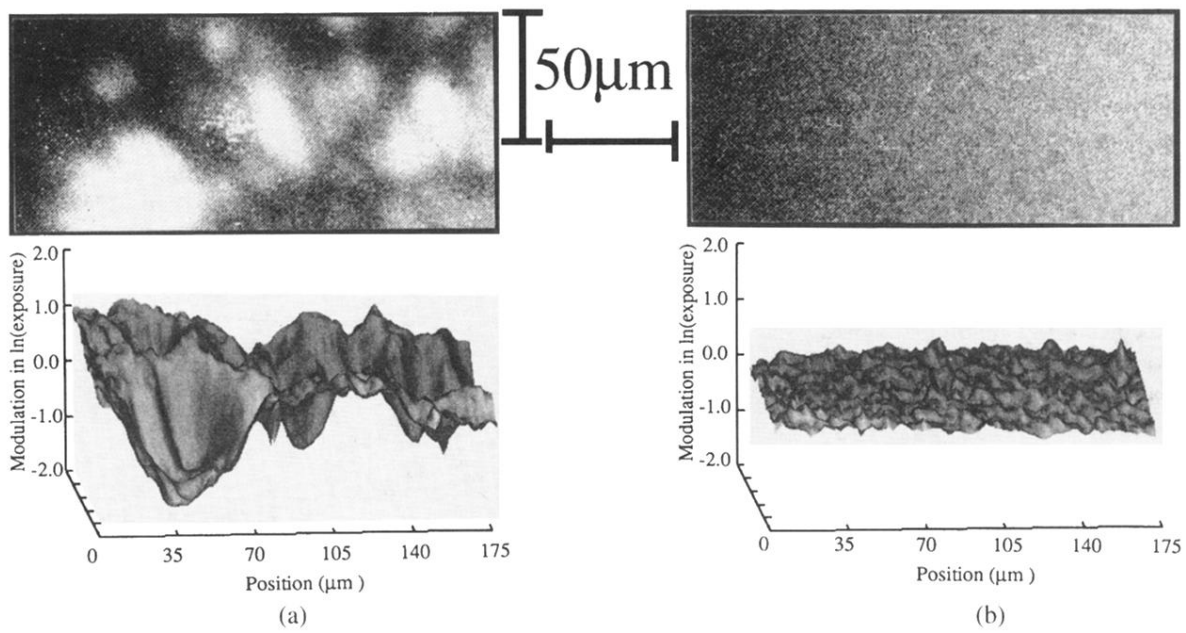


FIG. 2. Face-on 2D XUV radiographs and corresponding modulations in  $\ln(\text{exposure})$  across (a) a conventional,  $10.6 \mu\text{m}$  thick solid  $\text{C}_8\text{H}_8$  foil target, (b) an “FDD” target consisting of a gold-coated,  $50 \mu\text{m}$  thick triacrylate foam layer on a  $10.6 \mu\text{m}$  thick solid  $\text{C}_8\text{H}_8$  foil. These measurements were taken at  $2.1 \pm 0.2 \text{ ns}$  and sample one quarter of the focal spot profile of a coherent beam. Peak irradiance was  $(1.0 \pm 0.5) \times 10^{14} \text{ W cm}^{-2}$ .